Turkish Computational and Theoretical Chemistry

Turkish Comp Theo Chem (TC&TC)

Volume(Issue): 9(2) – Year: 2025 – Pages: 96-110

e-ISSN: 2602-3237

https://doi.org/10.33435/tcandtc.1518215

Received: 18.07.2024 ***Accepted***: 18.08.2024 *Research Article*

Unlocking the therapeutic potential of nolatrexed in glioblastoma multiforme through quantum mechanics, network pharmacology, molecular docking and ADMET analysis.

Aswin Krishnamurthy, Shabna Roupal Morais[1],

Department of Pharmaceutical Chemistry, Sri Ramachandra Faculty of Pharmacy, Sri Ramachandra Institute of Higher Education and Research, Porur, Chennai-600 116, (Tamilnadu) India

Abstract: Glioblastoma multiforme (GBM) is a highly aggressive brain tumor that remains challenging to treat due to its resistance to conventional therapies. In-silico investigations were conducted to analyse nolatrexed interactions with GBM targets using network pharmacology which identifies potential targets. The target nolatrexed was optimised and geometry was calculated for the Frontier molecular orbitals (FMO) and visualised using the 6-311(+)G(d)(p) basis set in Gauss View 16. Autodock tools 1.5.7 used for molecular docking, and the results were subsequently validated using Discovery Studio 4.5. ADMET analysed through ADMETlab 2.0, druglito and toxicity estimation software tool (T.E.S.T). In this study, FMO calculation was performed using Gaussian software were HOMO and LUMO ranges from 2.7059 to 7.9185 eV and shows higher energy gap signifies greater stability and lower reactivity The potential molecular targets of nolatrexed were first identifed using the Swiss Target Prediction platform and pathogenic targets of GBM were identifed using the Genecard, DisGeNET, and CTD database. Followed by compound and disease target overlapping, 69 targets were placed in that JUN, HSP90AA1, STAT3, MTOR, HSP90B1, IGF1R, GSK3B, JAK2, MAP2K1, and SIRT1 were the top-ranked target, which was estimated by CytoHubba plug-in. The molecular docking was performed for nolatrexed towards top 3 genes include mTORC1, mTORC2 and MAP2K1 from the PDB:7YRJ, 7TZO, 5HZE target. The binding score of nolatrexed were – 8.04 kcal/mol and – 7.2 kcal/ mol and -7.69 kcal/ mol respectively. Our findings, suggests that nolatrexed demonstrates potential binding affinity to mTORC1, mTORC2, and MAP2K1, which are the key targets associated with glioblastoma. Therefore it could be a promising candidate for further investigation in GBM treatment strategies.

Keywords: Gliomas, Brain tumor, anti-cancer, nolatrexed, network pharmacology.

1. Introduction

An estimated 5–6 primary malignant brain tumor cases are diagnosed annually per 100,000 people, with malignant gliomas (MGs) accounting for about 80% of these cases [1]. Over 30% of all the principal central nervous system (CNS) tumors are MGs, the most prevalent type of tumor derived from glial cells. They bear a major share of the blame for the death rates from brain tumors [2-4]. Survival rates for MGs have not significantly improved despite the limited treatment options available, particularly when compared to other cancers like lung and breast cancer. Considering several negative traits, the subcategories of malignant gliomas are based on the following factors: the abnormal appearance of the cell nuclei, proliferative capacity, the death of body tissue, vascular proliferation, mitotic activity, clinical course, and treatment result [5-9].

I, II, III, and IV grades of gliomas are among the most recent classifications of gliomas provided by the CNS WHO. These grades are used in clinical settings to help patients receive the right treatment. While grade II tumors have a limited capacity for proliferation, they are invasive and often occur again, tumors that are grade I have low

[1] Corresponding Authors

e-mail: shabnaroupal@sriramachandra.edu.in

multiplication rates and can be healed with surgery alone. Grade IV gliomas are the most advanced grade, have the worst prognosis, and have a high chance of being fatal. Grade III tumors are malignant, exhibiting the loss of the mature or specialized features of a cell or tissue and rapid mitotic cell division [10-13]. 90% of cases are Isocitrate dehydrogenase (IDH-wildtype), while the remaining 10% are IDH-mutant are the two subtypes of glioblastomas. IDH-mutant glioblastomas are more frequently found in younger patients and are linked to a history of previous lower-grade diffuse gliomas, whereas IDH-wildtype glioblastomas are typically found in patients over 55 [14-16].

Glioblastoma still has no known cure, despite ongoing research efforts. Current treatment option for glioblastoma include surgery, radiation and chemotherapy [17-20]. Increased cell proliferation, inhibition of apoptosis, invasion, and angiogenesis are all caused by these genetic abnormalities, which mainly interfere with the control of two important cellular systems: the cell cycle and growth factor-mediated signaling pathways [21]. Sometimes malignant cells become incapable of compensating for their loss of signaling through constitutively activated pathways. Thus, it might be possible to target cancer cells specifically and prevent them from growing and surviving while protecting healthy cells. Many studies have concentrated on finding genetic changes in GBMs that can be used to categorize patient subgroups with varying prognoses and/or responses to particular therapies.

Nolatrexed is an antineoplastic quinazoline moiety that is lipophilic and soluble in water. Clinical trial NCT00012324 Nolatrexed Dihydrochloride Compared With Doxorubicin in Treating Patients With Recurrent or Unresectable Liver Cancer is under investigation [22-25]. Moreover the drug nolatrexed can be used alongside of radiation therapy which suppress the tumor growth. Using computer modeling with Gaussian 16 software, the chemical properties of the nolatrexed was examined. Network pharmacology was performed and top 3 targets were selected for the treatment of Glioblastoma multiforme(GBM). Autodock and Biovia Discovery Studio 4.5 are used to perform molecular docking, tests against three proteins linked to glioblastoma that were redeemed from the Protein Data Bank (PDB). Structure of nolatrexed is depicted in the **Figure 1**.

2. Computational Method

2.1. Computational details:

The initial geometry of nolatrexed was obtained from the PubChem online structure database. The optimization of geometry and subsequent modifications to all structures were performed using the Gaussian 09 software. Six (6) functionals, namely B3LYP, B3PW91, CAM-B3LYP, MPWIPW91, PBEPBE, and WB97XD, implemented in Gaussian16 software, were employed to optimize the structure of the compound. The geometry was visualized using the 6-311(+)G(d)(p) basis set in Gauss View 16 and Frontier molecular orbital (FMO) calculation was performed.

2.2. Target prediction of nolatrexed against GBM

Using swiss Target Prediction database (http://www.swisstargetprediction.ch/) the potential targets for nolatrexed was predicted [26]. From PubChem database (https://pubchem.ncbi.nlm.nih.gov/) the canonical smiles were obtained and were uploaded to the swiss Target Prediction server. To standardize the uniport ID to the gene symbols, species “Homo sapiens” were selected. At the same time, the targets GBM were predicted in the GeneCards (https://www.genecards.org/) [27] , DisGeNet database (https://www.disgenet.org/home/) [28], and Comparative Toxicogenomics Database (CTD) (https://ctdbase.org/) [29]. The keyword “ Glioblastoma multiforme” were used to collect potential genes. Subsequently further analysis was performed by overlapping the component targets and GBM targets using the Venn diagram which represented the potential targets of Nolatrexed against GBM.

2.3. Gene ontology and KEGG pathway enrichment analysis

Nolatrexed in treatment of GBM, the core mechanism and pathway was explored by GO function and KEGG pathway enrichment analysis. Hub genes obtained from the overlapping was searched in the ShinyGO 0.80 (http://bioinformatics.sdstate.edu/go/) by limiting

the species to "Homo sapiens". Biological process (BP), cell components (CC), molecular function (MF), and KEGG pathways were collected [30].

2.4. Construction of the compound-target network

For network construction and visualization, Cytoscape 3.8.2 (https://cytoscape.org/) was employed, allowing analysis of biomolecular interaction networks. The chemical compounds and target genes were represented as nodes in the network representation, and the interactions between the chemical compounds and their target genes were shown as edges [31].

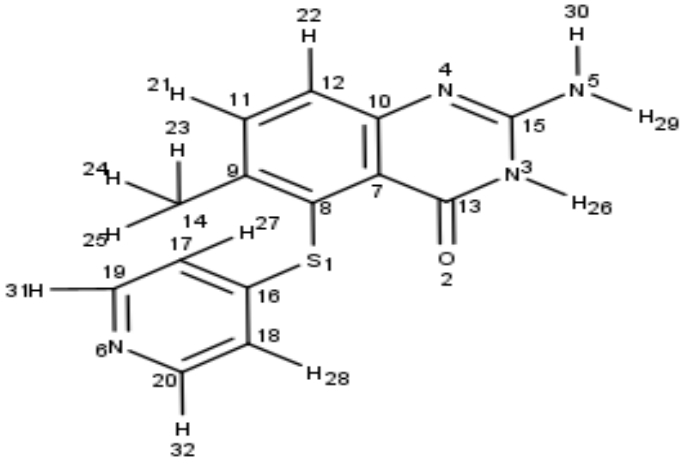

Figure 1: Structure of Nolatrexed

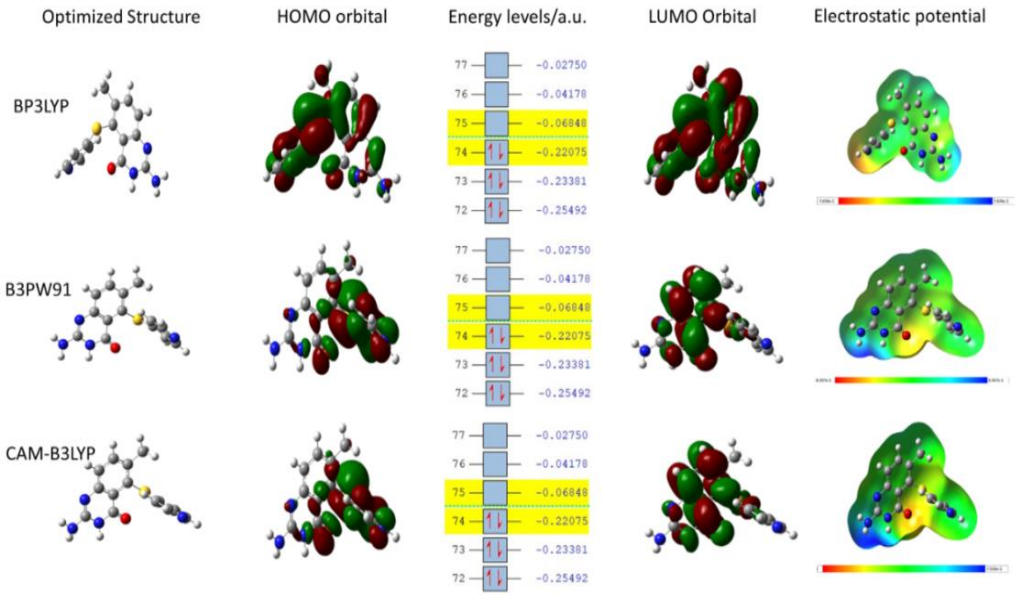

Figure 2(a): Optimized structure with HOMO and LUMO orbitals, energy levels, and electrostatic potential of Nolatrexed at B3LYP, B3PW91, CAM-B3LYP.

2.5. Protein-protein interaction (PPI) network construction

The STRING (http://string-db.org; Version 12.0) database was used to construct a protein-protein interaction (PPI) network for nolatrexed in treatment of GBM to analyze the functional interaction between proteins. The network confdence score ≥0.4 was set to obtain targets with "Homo sapiens" being selected in Cytoscape sofware (version 3.8.2) further. Using the Cyto-Hubba plug-in Cytoscape software, the top-ranked targets were scrutinized by the means of selecting the top 10 Hubba nodes using Maximal Clique Centrality (MCC) ratio.

2.6. Molecular docking

In contrast, the target protein was obtained by evaluating the resolution and release time in the Protein Data Bank (PDB) (www.rcsb.org) website, and nolatrexed chemical structure were downloaded from the PubChem database. The docking was performed using Autodock Tools 1.5.7 [32]. The 3-D and 2-D structures were generated using Biovia Discovery studio software 4.5. In this study the molecular docking of nolatrexed was carried towards the PDB ID: 7JRJ, 7TZO, and 5HZE.

2.7. ADMET

ADMETlab 2.0 (https://admetmesh.scbdd.com/) and Druglito (https://niper.gov.in/pi_dev_tools/DruLiToWeb/DruLiTo_index.html) were used for determining the pharmacokinetic parameters [33,34]. The US Environmental Protection Agency offers free software called Toxicity Estimation Software Tool (T.E.S.T.) was used for toxicity analysis for Nolatrexed [35].

3. Results and discussion

3.1. Frontier Molecular Orbital (FMO) Analysis:

The lowest molecular orbital (LUMO) and the highest occupied molecular orbital (HOMO) together form the frontier molecular orbital (FMO) [36], which is illustrated in **Figure 2(a) and 2(b)** below. **Table 1** exhibits the quantum attributes of nolatrexed. The HOMO values span from -5.9669 to -7.9223 eV. The energy gap, derived by the contrast allying the HOMO and LUMO, elucidates the stability and reactivity of the nolatrexed, which ranges from 2.7059 to 7.9185 eV and shows higher energy gap signifies greater stability and lower reactivity. Besides these descriptors, other DFT quantum chemical descriptors are electronegativity (χ), electrophilicity index (ω), softness (s), hardness (η), and maximum charge transfer (Nmax). These descriptors are calculated using equations (1) to (6). The χ (Chemical Hardness) range encompasses 3.8637 to 4.0365 eV, indicating the nolatrexed resilience to alterations in electron density. The η (Chemical Softness) range encompasses 1.3529 to 3.9592 eV, with higher values signifying an increased inclination for electron donation. The μ (dipole moment) range spans from 1.5663 to 6.1310 Debye, exemplifying the polarity of the nolatrexed which depicts greater values indicate a more polar nature. The electrophilicity index (ω), determined as per equation (6), ranges from 1.9834 to 3.7296 eV, with lower values indicating stronger electrophilicity. The N_{max} , D_{En} , and D_{Ee} are calculated using the equation (7, 8, 9).The ΔNmax (Maximum Charge Transfer) range spans from 1.0009 to 2.8559, signifying the utmost extent of charge that can be transferred.

$$I = -EHOMO \quad (1)$$

$$A = -ELUMO \quad (2)$$

$$\chi = -\mu = \frac{I + A}{2} \quad (3)$$

$$\eta = \frac{I - A}{2} \quad (4)$$

$$S = \frac{1}{2\eta} \quad (5)$$

$$\omega = \frac{\mu^2}{2\eta} \quad (6)$$

$$N_{max} = \frac{\mu}{\eta} \quad (7)$$

$$D_{En} = -A + w = \frac{(\mu + \eta)^2}{2\eta} \quad (8)$$

$$D_{Ee} = I + w + = \frac{(\mu - \eta)^2}{2\eta} \quad (9)$$

The ΔEn (net electronegativity) range lies between 1.732 and 3.006, indicating the overall tendency of the compound to form ionic or polar covalent bond. Lastly, the ΔEe (Chemical Potential) range extends from 9.5362 to 10.734, representing the molecule move from higher to lower chemical potential by releasing some amount of energy. Identification of electrophilic and nucleophilic attack sites is enabled by electrostatic potential examination.

3.2. Network pharmacology

Comparing the targets of nolatrexed against Glioblastoma multforme: The targets for GBM were identified in the GeneCard, DisGeNET, and CTD databases, with a total of 7917 (39, 3197, and 4681), respectively. Out of these three types of

databases, 6384 GBM targets were found after removing duplicate entries. We obtained 100 potential nolatrexed targets based on SwissTarget prediction. A Venn plot depicting the intersection of the GBM disease targets and the nolatrexed targets produced 69 potential targets for GBM treatment (Figure 3). Figure 4 shows the hub gene network analysis. Figure 5 illustrates the construction of the hub gene network.

3.3. Protein−Protein Interaction (PPI) Data

Cytoscape software was used to visualize and arrange the interactions between the final target proteins, which were carried out using the online complex protein database STRING. With 69 nodes and 629 edges, the PPI network had an average node degree of 18.2 and an average clustering coefficient of 0.656. The PPI network was constructed and modified at medium confidence (0.400). An enrichment of PPI with a P-value less than 1.0 × 10−16 is considered significant. The top ten core targets, including JUN, HSP90AA1, STAT3, MTOR, HSP90B1, IGF1R, GSK3B, JAK2, MAP2K1, and SIRT1, were identified through network analysis of the top targets (Figure 6).

3.4. Gene ontology function and KEGG pathway enrichment analysis

Using the ShinyGO database, we constructed a network of all hit genes targeted by nolatrexed when interacting with various defined targets, with the aim of developing a target gene-pathway networking. The P13K-AKT and m-TOR signaling pathways are the focus of the pathway analysis presented in the KEGG diagram. The KEGG-labeled diagram Figure 7A shows that m-TOR and MAP2K1 are primarily responsible for the majority of the genes in the anticancer pathways. Figure 7 B, C, D depict the gene ontology functions for biological, cellular, and molecular processes. Specifically, the top three biological processes are regulation of cellular response to heat (GO:1900034), axon development (GO:0048699), and response to organonitrogen compound (GO:0010243). The molecular function includes sulfonylurea receptor binding (GO:0017098), adenyl deoxyribonucleotide binding (GO:0032558), protein serine/threonine/tyrosine kinase activity (GO:0004712), and axonal development cones (GO:0044295), sperm plasma membrane (GO:0097524), and dendritic growth cones (GO:0044294) are the next cellular components.

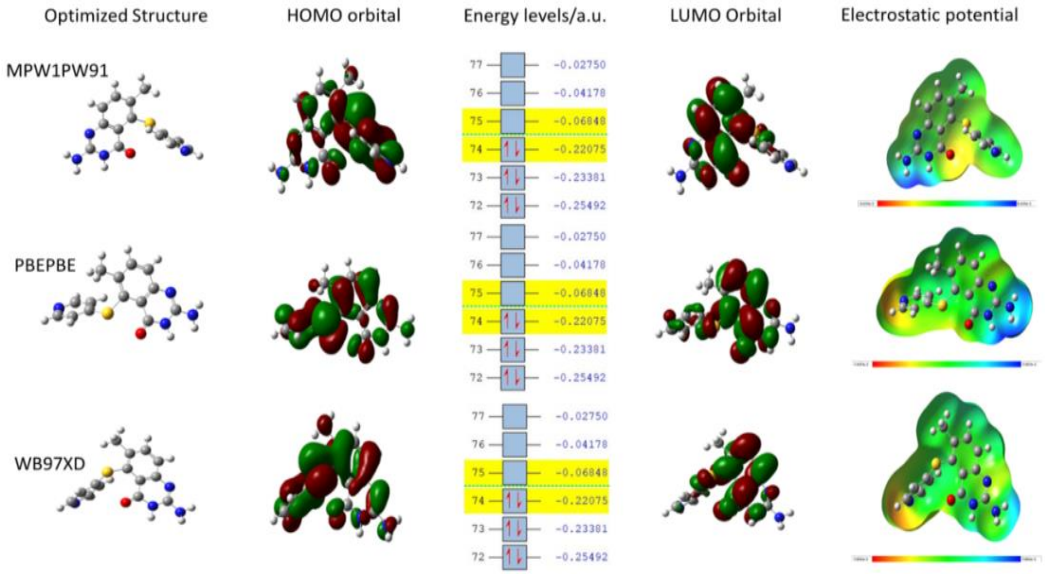

Figure 2(b): Optimized structure with HOMO and LUMO orbitals, energy levels, and electrostatic potential of nolatrexed.

Table 1. Quantum descriptors of nolatrexed

Quantum descriptors (eV)	B3LYP	B3PW91	CAM-B3LYP	MPWIPW91	PBEPBE	WB97XD
ELUMO	-1.8634	-1.8626	-0.6767	-1.6531	-2.5108	-0.0038
EHOMO	-6.0069	-5.9669	-7.3963	-6.1511	-5.2167	-7.9223

ELUMO+1	-1.1369	-1.0753	0.0609	-0.8604	-1.8961	0.7409
EHOMO-1	-6.3623	-6.2747	-7.7335	-6.4447	-5.6434	-8.2782
I	6.0069	5.9669	7.3963	6.1511	5.2167	7.9223
A	1.8634	1.8626	0.6767	1.6531	2.5108	0.0038
Energy gap 1	4.1435	4.1043	6.7196	4.498	2.7059	7.9185
Energy gap 2	5.2254	5.1994	7.6726	7.6726	3.7473	7.5373
χ	3.9309	3.9147	4.0365	3.9021	3.8637	3.9630
η	2.0716	2.0522	3.3598	2.249	1.3529	3.9592
ω	3.7296	3.7338	2.4247	3.3851	5.5171	1.9834
S	0.2413	0.2436	0.1488	0.2223	0.3696	0.1262
μ	-3.9309	-3.9147	-4.0365	-3.9021	-3.8637	-3.9630
ΔNmax	1.8975	1.90764	1.2014	1.7350	2.8559	1.0009
ΔEn	1.8662	1.8712	1.748	1.732	3.006	1.9796
ΔEe	9.7365	9.7007	9.821	9.5362	10.734	9.9057
Dipole moment (Debye)	5.7164	6.1310	1.5663	6.0496	5.3759	5.5228

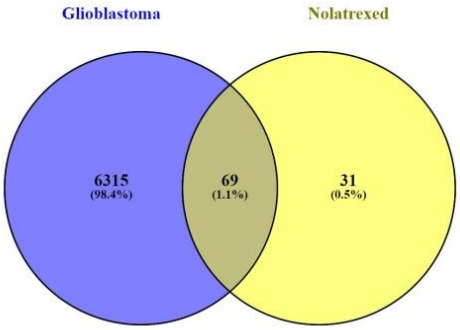

Figure 3. Nolatrexed- Glioblastoma target venn plot

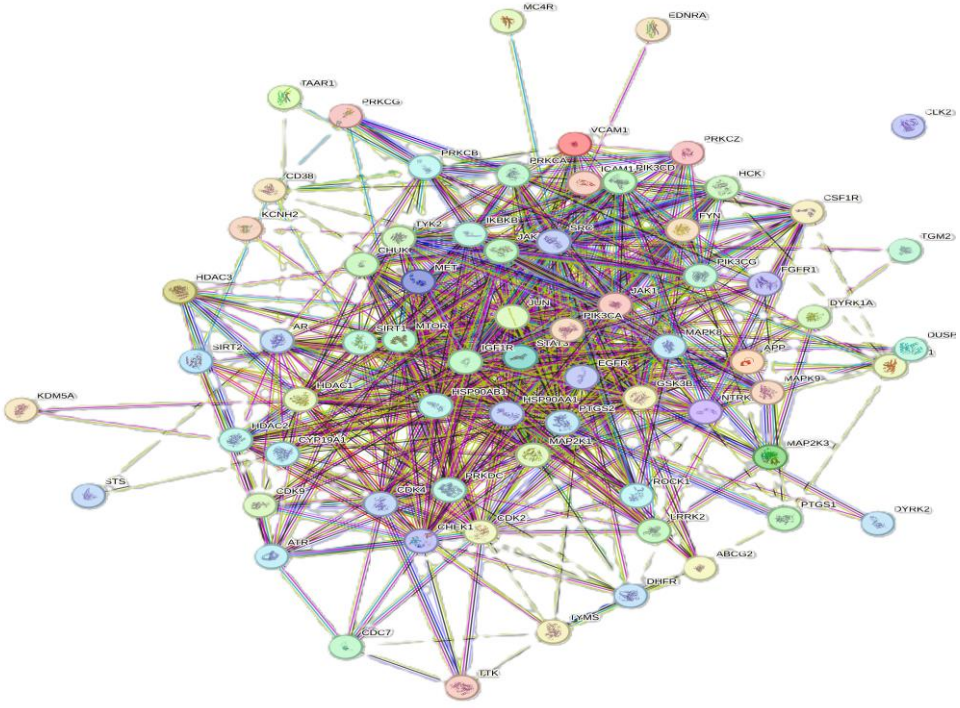

Figure 4. Hub gene network analysis

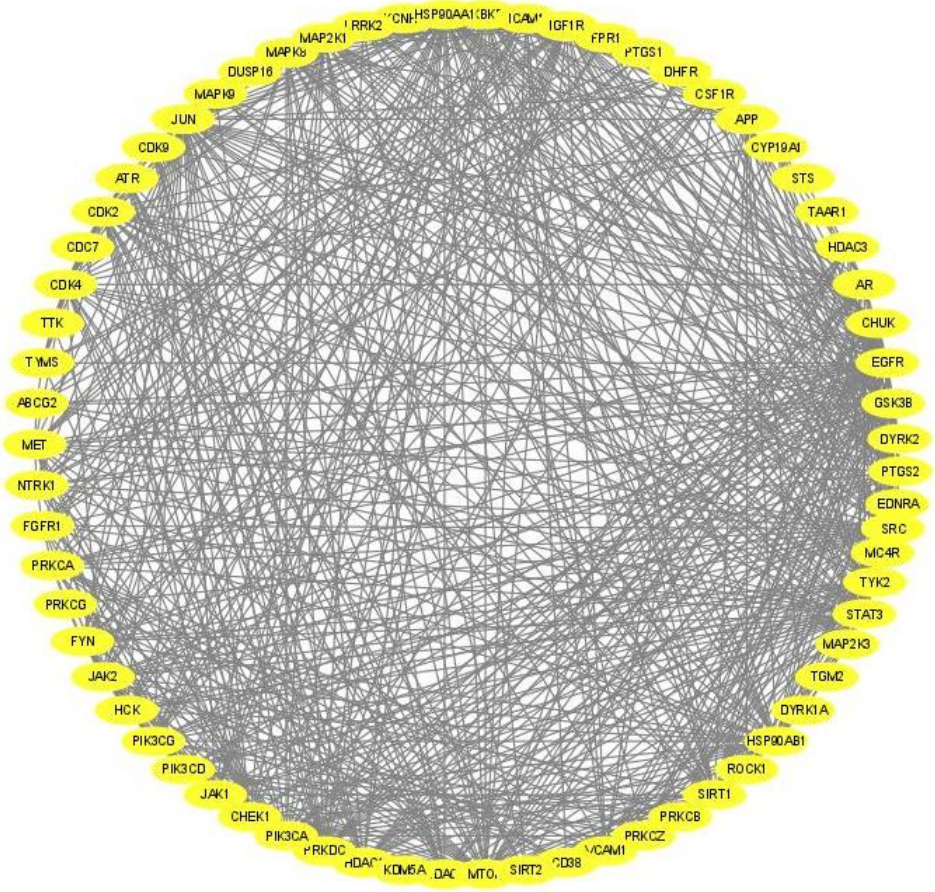

Figure 5. Construction of the hub gene network

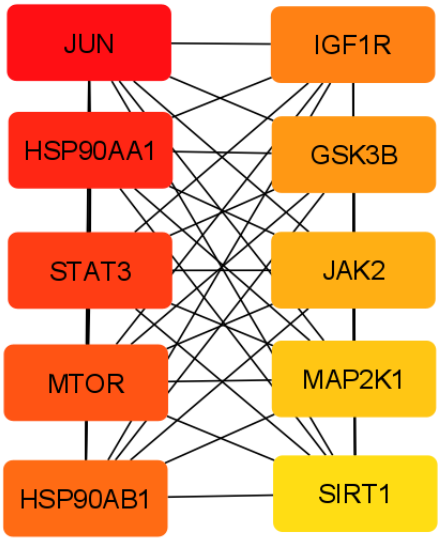

Figure 6. Analysis of the top-ranked targets' networks. (Orange signifies -moderate interactive; yellow indicates -mild interactive; red represents top order -highly interactive.)

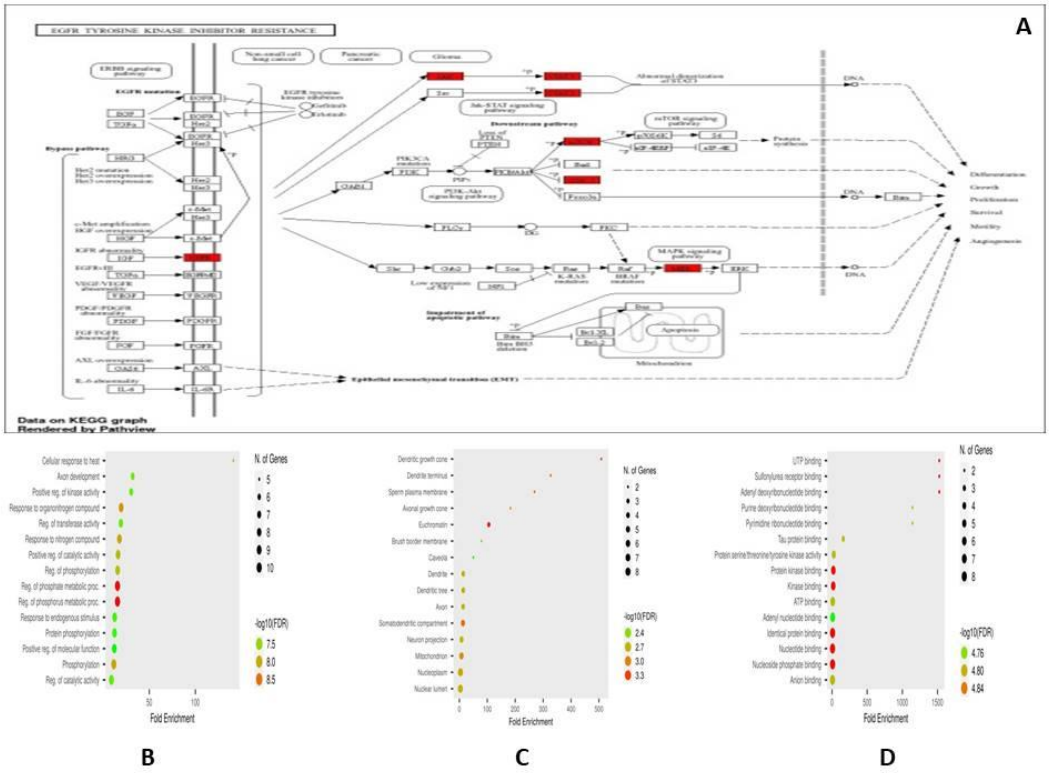

Figure 7. A: EGFR tyrosine kinase inhibitor resistance. The red mark represents enrichment of the target of nolatrexed in the EGFR tyrosine kinase inhibitor resistance pathway, B: Biological process, C: cellular component, D: Molecular function

Table 2. Binding affinities and interactions of nolatrexed with target proteins

S.No	Target	Protein Databank	Binding affinities (kcal/mol)
1.	mTORC1	7YRJ	-8.04
2.	mTORC2	7TZO	-7.2
3.	MAP2K1	5HZE	-7.69

Mammalian target of rapamycin (mTOR) is an essential signalling mechanism that controls growth, proliferation, metabolism, and survival of cells, among other biological functions. It is essential for functioning and controlling vital cellular processes necessary for tumour development and survival hence mTOR is the therapeutic target for glioblastoma. mTOR signalling pathway consists of two protein complexes mTORC1 and mTORC2. Both play a major role in regulating protein synthesis, cell survival, and cytoskeletal oraganisation and cell growth [37]. Nolatrexed has the highest binding affinity with mTORC1 (D chain of 7YRJ) of -8.04 kcal/mol with PRO203, MET202, LEU164, ASP162, PHE163, ALA161, VAL131, LEU149, ASP150, GLY132, LEU198, LEU151, TYR201 amino acid residues as compared with mTORC2 (E chain of 7TZO) of -7.2 kcal/mol with ARG1609, ASP1649, ILE1650, LEU1537, CYS1651, GLN1684, PHE1682, LEU1683, ASP1648, SER1538 amino acid residues depicted in figure 8 and 9. Common genetic alterations that can activate the mTOR signalling pathway include the deletion of the tumour suppressor gene PTEN. Patients with intact PTEN may respond more favourably to mTOR inhibitors because the pathway is not as hyperactivated. Hence it can inhibit the both the complexes of mTOR signalling pathway and exhibit good therapeutic target for glioblastoma. Improving patient outcomes and upsetting a variety of carcinogenic processes are possible effects of mTOR inhibition. The other effect which produced by inhibiting mTOR include induce autophagy thereby increasing protein degradation. The combination of autophagy inhibitors with mTOR

inhibitors has the potential to increase therapeutic success by sensitising glioblastoma cells to mTOR inhibition [38,39]. By combining mTOR inhibitors with inhibitors of the MAPK/ERK pathway, therapeutic effectiveness may be increased and resistance may be overcome. Increased GBM cell growth, proliferation, and migration are caused by the activation of pro-survival and mitogenic mediators Akt and ERK1/2 thereby activating mTORC1 and increase protein synthesis. Conversely, AKT functions as a downstream effector of mTORC2 and contributes to the growth and survival of cells. In preclinical settings, combining mTOR and AKT inhibitors has demonstrated potential in improving the therapeutic response and overcoming resistance.

Nolatrexed has the highest binding affinity with the protein 5HZE of -7.69 kcal/mol with CYS207, LYS97, MET143, HIS145, LEU197, MET146, VAL82, MET146, ALA95, GLU144, LEU74, GLY149, ASP147, GLY75 amino acid residues depicted in figure 10. It exerts the inhibitory effect on the MAP2K1, which is the major therapeutic target for GBM [40-43]. The decrease in MAPK3 (also known as ERK1) and MAP2K1 (also known as MEK), also leads to a decrease in the ability to activate RSK which regulates LKB1, an AMPK activator, by phosphorylation and TSC1/2 thereby preventing the activation of Rheb hence no formation of mTORC1. The MAPK3 which is activated by MAP2K1 is inhibited and cause decrease cell proliferation, survival and metastasis. By combining mTOR inhibitors with inhibitors of the MAPK/ERK pathway, therapeutic effectiveness may be increased and resistance may be overcome.

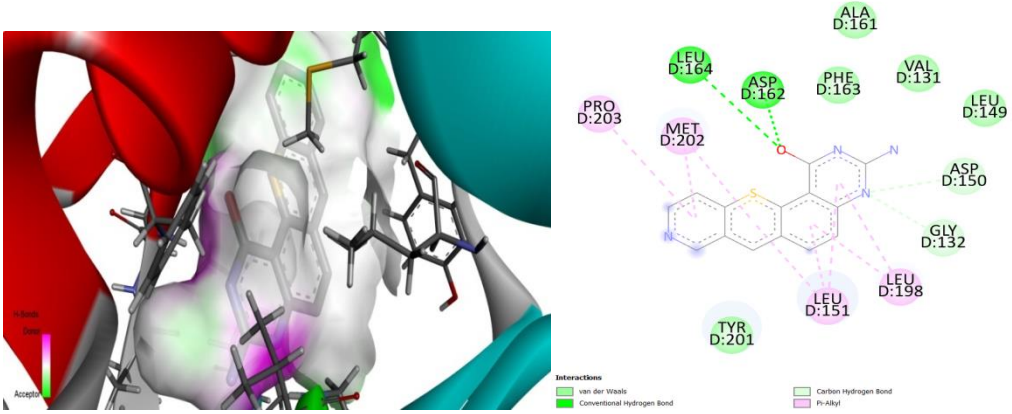

Figure 8. 2-D and 3-D image for nolatrexed compound interaction with mTORC1 (PDB: 7YRJ D CHAIN)

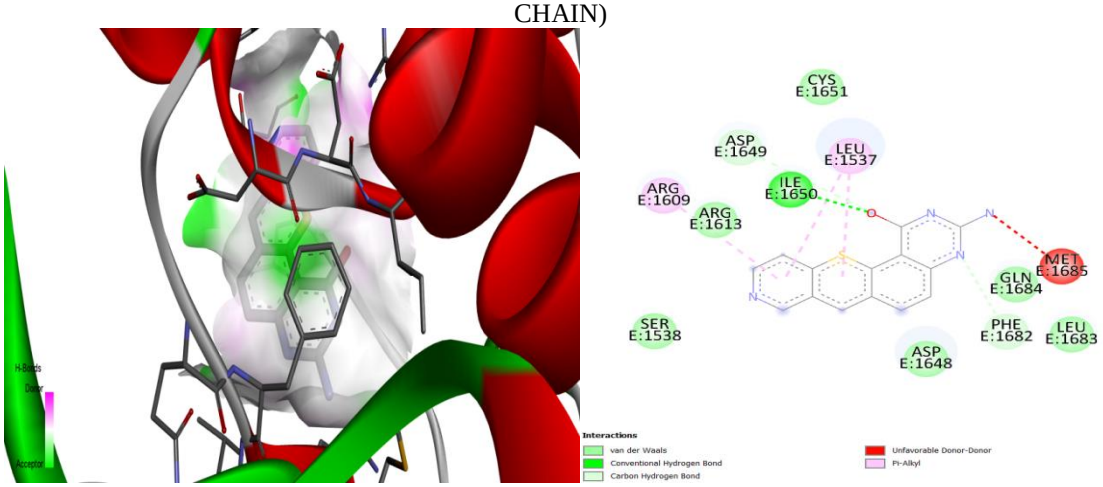

Figure 9. 2-D and 3-D image for nolatrexed compound interaction with mTORC2 (PDB: 7ZTO E CHAIN)

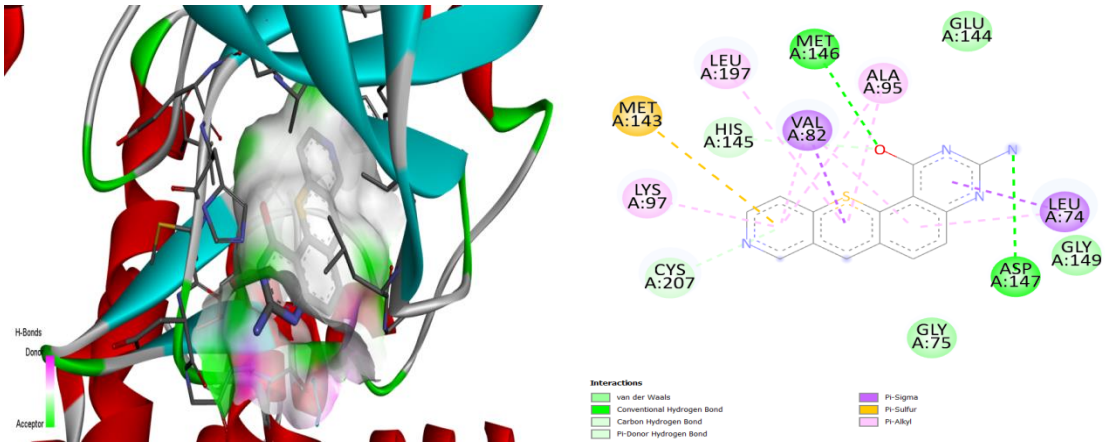

Figure 10. 2-D and 3-D image for nolatrexed compound interaction with MAP2K1 (PDB: 5HZE A CHAIN)

3.5. ADMET

The design of computational drugs heavily relies on the ADMET study to determine drug ability by analyzing molecular characteristics. Specific criteria such as molecular weight, log P values, and hydrogen bond counts are used to evaluate drug-likeness. **Table 3** shows drug ADMET properties of nolatrexed using ADMETlab 2.0.Orally taken drugs primarily absorbed in stomach. It has good oral bioavailability and crosses the Blood brain barrier (BBB) effectively. Nolatrexed interacts with CYP450 1A2 as a substrate and inhibitor, but not with CYP450 3A4. It is neither a substrate nor an inhibitor for CYP450 2C9, 2C19, and 2D6. It has a 1.633-hour half-life, which is short and suggests that the body eliminates it quickly. The poor clearance rate (1.148 mL/min/kg) points to delayed drug clearance. It shows non-mutagenicity, low acute toxicity, and non-sensitizing attributes. However, drug-induced liver damage raises concerns. LD50 for nolatrexed is 929.57 mg/kg, posing risk to rats.

Table 3. ADMET analysis of nolatrexed

Physicochemical Property		
LogS (Solubility)	-3.87log mol/L	Low solubility
LogD (Distribution coefficient D at pH = 7.4)	1.631	Solubility is moderate; permeability is moderate; and metabolism is low.
LogP (Distribution coefficient P)	2.36	poor aqueous solubility.
Absorption		
Caco-2- permeability	-4.777cm/s	Optimal
Pgp-inhibitor	0.083	Non-inhibitor
Pgp-substrate	0.036	Non-substrate
HIA (human intestinal absorption)	0.684	HIA+
F (20% Bioavailability)	0.746	F20+
F (30%Bioavailability)	0.546	F30+
Distribution		
PPB (plasma protein binding)	83.356%	Moderate protein-bound and therapeutic index.
BBB (Blood-brain-barrier)	0.873	BBB+
VD (Volume distribution)	-0.404 L/kg	Evenly distributed

Metabolism		
CYP450 1A2 inhibitor	0.587	Inhibitor
CYP450 1A2-substrate	0.624	Substrate
CYP450 3A4 inhibitor	0.803	Inhibitor
CYP450 3A4 substrate	0.326	Non-substrate
CYP450 2C9 inhibitor	0.296	Non-inhibitor
CYP450 2C9 substrate	0.266	Non-substrate
CYP450 2C19 inhibitor	0.584	Inhibitor
CYP450 2C19 substrate	0.46	Non-substrate
CYP450 2D6 inhibitor	0.407	Non-inhibitor
CYP450 2D6 substrate	0.26	Non-substrate
Excretion		
T1/2 (Half-life)	1.633 hour	low
Cl (Clearance)	1.148mL/min/kg	low
Toxicity		
hERG (hERG blockers)	0.315	Non-blockers
H-HT (Human hepatotoxicity)	0.862	HT positive (+)
Ames (Ames mutagenicity)	0.374	Ames negative (-)
SkinSen (Skin sensitization, (r)LLNA)	0.267	Non-sensitizer
LD50 (LD50 of acute toxicity)	2.449(-log mol/kg)	Low toxicity
DILI (Drug-induced liver injury)	0.964	DILI positive (+)
FDAMDD (Maximum recommended daily dose)	0.64	FDAMDD positive(+)

Table 4: Pharmacokinetic activities using Druglito

Properties	**Druglito**
MW	284.07
Log P	-0.368
Alog P	0.03
HBA	5
HBD	2
TPSA	105.14
AMR	83.32
nRB	2
nAtom	32

nAcidic group	0
RC	3
nRigid B	20
nArom ring	2
nHB	7

Table 5: The estimated toxicity values of nolatrexed using TEST Version 4.2

Parameters	**Toxicity values**
LC50 (96 h) (mg/L)	-
LD50 (mg/kg)	929.57
Developmental toxicity	0.73(+)
Ames mutagenicity	0.42(-)

Note: LD50 is the quantity of drug in mg/kg of body weight that results in the demise of 50% of rats after being administered orally. "+" indicates a positive result, while the "-" indicates a negative result. On the other hand, LC50 (96 h) is the test drug concentration in water (mg/L) that causes the demise of 50% of fathead minnows after 96 hours.

4. Conclusions

Glioblastoma multiforme (GBM), a very aggressive kind of brain tumour, can be treated with nolatrexed, a strong antineoplastic drug from the quinazoline family. By focusing on important biochemical pathways linked to the development of GBM, nolatrexed has demonstrated considerable therapeutic potential. Computer tools, such as network pharmacology analysis and molecular docking studies, have clarified how nolatrexed interacts with certain targets that are important to the pathogenesis of GBM. These studies have identified molecular targets such as mTOR, MAP2K1, involved in cell signaling and survival pathways. Additionally, nolatrexed as a targeted treatment for GBM has been highlighted by binding affinity studies, which have further demonstrated its capacity to successfully engage with these targets. Similarly, assessments of pharmacological properties of nolatrexed using ADMET prediction models suggest favorable drug characteristics, supporting its further exploration in preclinical and clinical trails. As a result, continued research and clinical trials are essential to validate efficacy and safety profile of nolatrexed as a potential therapeutic option in the challenging landscape of GBM treatment.

Author Contribution:

Methodology, Resources, Investigation, Writing-Original draft preparation, Validation, Supervision, Writing-Reviewing and Editing are all responsibilities of Aswin K and Shabna Roupal Morais.

Declaration of competing interest:

The authors confirm that no conflicting financial interests or personal ties that may have impacted the work described in this publication have come to their knowledge.

Acknowledgement:

The administration of Sri Ramachandra Faculty of Pharmacy, Sri Ramachandra Institute of Higher Education and Research in Tamilnadu is thanked for their assistance and encouragement.

References

[1] C. Alifieris, D.T. Trafalis, Glioblastoma multiforme: Pathogenesis and treatment, Pharmacology & therapeutics 152 (2015) 63-82.

[2] M. Martín-Landrove, F. Torres-Hoyos, A. Rueda-Toicen, Complexity of brain tumors, Physica A: Statistical Mechanics and its Applications 537 (2020) 122696.

[3] H. Ohgaki, P. Dessen, B. Jourde, S. Horstmann, T. Nishikawa, P.L. Di Patre, C. Burkhard, D. Schuler, N.M. Probst-Hensch, P.C. Maiorka, N. Baeza, Genetic pathways

to glioblastoma: a population-based study, Cancer research 64 (2004) 6892-6899.

[4] K. Anjum, B.I. Shagufta, S.Q. Abbas, S. Patel, I. Khan, S.A. Shah, N. Akhter, S.S. ul Hassan, Current status and future therapeutic perspectives of glioblastoma multiforme (GBM) therapy: A review, Biomedicine & Pharmacotherapy 92 (2017) 681-689.

[5] C. Pasqualini, T. Kozaki, M. Bruschi, T.H. Nguyen, V. Minard-Colin, D. Castel, J. Grill, F. Ginhoux, Modeling the interaction between the microenvironment and tumor cells in brain tumors Neuron 108 (2020) 1025-1044.

[6] C.L Tso, W.A. Freije, A. Day, Z. Chen, B. Merriman, A. Perlina, Y. Lee, E.Q. Dia, K. Yoshimoto, P.S. Mischel, L.M. Liau, Distinct transcription profiles of primary and secondary glioblastoma subgroups, Cancer research 66 (2006) 159-167.

[7] R.M. Young, A. Jamshidi, G. Davis, J.H. Sherman, Current trends in the surgical management and treatment of adult glioblastoma Annals of translational medicine 3 (2015).

[8] J.R. Henry, M.M. Mader, Recent advances in antimetabolite cancer chemotherapies, Annual reports in medicinal chemistry 39 (2004) 161-172.

[9] T. Aoki, N. Hashimoto, M. Matsutani, Management of glioblastoma, Expert opinion on pharmacotherapy 8 (2007) 3133-3146.

[10] V. Rajaratnam, M.M. Islam, M. Yang, R. Slaby, H.M. Ramirez, S.P. Mirza, Glioblastoma: Pathogenesis and current status of chemotherapy and other novel treatments, Cancers 12 (2020) 937.

[11] C. Lei, P. Davoodi, W. Zhan, P.K. Chow, C.H. Wang, Development of nanoparticles for drug delivery to brain tumor: the effect of surface materials on penetration into brain tissue, Journal of Pharmaceutical Sciences 108 (2019) 1736-1745.

[12] A. Lupton, H. Abu-Suwa, G.C. Bolton, C. Golden, The implications of brain tumors on aggressive behavior and suicidality: a review, Aggression and violent behaviour 54 (2020) 101416.

[13] C. Wang, S. Sinha, X. Jiang, S. Fitch, C. Wilson, V. Caretti, A. Ponnuswami, M. Monje, G. Grant, F. Yang, A comparative study of brain tumor cells from different age and anatomical locations using 3D biomimetic hydrogels, Acta biomaterialia 116 (2020) 201-208.

[14] D.N. Louis, A. Perry, G. Reifenberger, A. Von Deimling, D. Figarella-Branger, W.K. Cavenee, H. Ohgaki, O.D. Wiestler, P. Kleihues, D.W. Ellison, The 2016 World Health Organization classification of tumors of the central nervous system: a summary Acta neuropathologica 131 (2016) 803-820.

[15] S. Ferguson, M.S. Lesniak, Percival Bailey and the classification of brain tumors, Neurosurgical focus 18 (2005) E8.

[16] S. Yamaguchi, H. Kobayashi, S. Terasaka, N. Ishii, J. Ikeda, H. Kanno, H. Nishihara, S. Tanaka, K. Houkin, The impact of extent of resection and histological subtype on the outcome of adult patients with high-grade gliomas, Japanese journal of clinical oncology 42 (2012) 270-277.

[17] V. Gilard, A. Tebani, I. Dabaj, A. Laquerriere, M. Fontanilles, S. Derrey, S. Marret, S. Bekri, Diagnosis and management of glioblastoma: A comprehensive perspective, Journal of Personalized Medicine 11 (2021) 258.

[18] M. Preusser, Matthias, S. De Ribaupierre, A. Wohrer, S.C. Erridge, M. Hegi, M. Weller, R. Stupp, Current concepts and management of glioblastoma, Annals of neurology 70 (2011) 9-21.

[19] T.C. Ryken, B. Frankel, T. Julien, J.J. Olson, Surgical management of newly diagnosed glioblastoma in adults: role of cytoreductive surgery, Journal of neuro-oncology (2008) 271-286.

[20] N. Sanai, M.S. Berger, Recent surgical management of gliomas, Advances in Experimental Medicine and Biology 746 (2012) 12-25.

[21] P.S. Mischel, T.F. Cloughesy, Targeted molecular therapy of GBM, Brain pathology 13 (2003) 52-61.

[22] S.H. Reich, S.E. Webber, Structure-based drug design (SBDD): Every structure tells a story..., Perspectives in Drug Discovery and Design 1 (1993) 371-390.

[23] W.M. Chen, S.H. Wan, New Straightforward Synthesis of 2-Amino-6-methyl-5-(pyridin-4-ylsulfanyl)-3 H-quinazolin-4-one, Synthetic communications, 37 (2007) 53-61.

[24] X. Zhao, F. Li, W. Zhuang, X. Xue, Y. Lian, J. Fan, D. Fang, A new method for synthesis of Nolatrexed dihydrochloride, Organic Process Research & Development 14 (2010) 346-350.

[25] G.G. Hall, Applications of quantum mechanics in theoretical chemistry, Reports on Progress in Physics 22 (1959) 1-30.

[26] A. Daina, O. Michielin, V. Zoete, iLOGP: a simple, robust, and efficient description of n-octanol/water partition coefficient for drug design using the GB/SA approach, Journal of chemical information and modelling 54 (2014) 3284-3301.

[27] G. Stelzer, N. Rosen, I. Plaschkes, S. Zimmerman, M. Twik, S. Fishilevich, T.I. Stein, R. Nudel, I. Lieder, Y. Mazor, S. Kaplan. The GeneCards suite: from gene data mining to disease genome sequence analyses, Current protocols in bioinformatics 54 (2016) 1-30.

[28] J. Piñero, J. Sauch, F. Sanz, L.I. Furlong, The DisGeNET cytoscape app: Exploring and visualizing disease genomics data, Computational and structural biotechnology journal 19 (2021) 2960-2967.

[29] A.P. Davis, T.C. Wiegers, J. Wiegers, B. Wyatt, R.J. Johnson, D. Sciaky, F. Barkalow, M. Strong, A. Planchart, C.J. Mattingly, CTD tetramers: a new online tool that computationally links curated chemicals, genes, phenotypes, and diseases to inform molecular mechanisms for environmental health, Toxicological Sciences 195 (2023) 155-168.

[30] S.X. Ge, D. Jung, R. Yao, ShinyGO: a graphical gene-set enrichment tool for animals and plants, Bioinformatics 36 (2020) 2628-2629.

[31] P. Shannon, A. Markiel, O. Ozier, N.S. Baliga, J.T. Wang, D. Ramage, N. Amin, B. Schwikowshi, T. Ideker, Cytoscape: a software environment for integrated models of biomolecular interaction networks, Genome research 13 (2003) 2498-2504.

[32] G.M. Morris, R. Huey, W. Lindstrom, M.F. Sanner, R.K. Belew, D.S. Goodsell, A.J. Olson, AutoDock4 and AutoDockTools4: Automated docking with selective receptor flexibility, Journal of computational chemistry 30 (2009) 2785-2791.

[33] G. Xiong, Z. Wu, J. Yi, L. Fu, Z. Yang, C. Hsieh, M. Yin, X. Zeng, C. Wu, A. Lu, X. Chen, ADMETlab 2.0: an integrated online platform for accurate and comprehensive predictions of ADMET properties, Nucleic acids research 49 (2021) W5-W14.

[34] G.R. Bickerton, G.V. Paolini, J. Besnard, S. Muresan, A.L. Hopkins, Quantifying the chemical beauty of drugs, Nature chemistry 4 (2012) 90-98.

[35] www.epa.gov/chemical-research/toxicity-estimation-software-tool-test, February 2024, Accessed:17.07.2024.

[36] D.R. Salahub, R. Fournier, P. Mlynarski, I. Papai, A. St-Amant, J. Ushio, Gaussian-based density functional methodology, software, and applications, In Density functional methods in chemistry, Springer New York (1991) 77-100.

[37] S. Singh, D. Barik, K. Lawrie, I. Mohapatra, S. Prasad, A.R. Naqvi, A. Singh, G. Singh, Unveiling novel avenues in mTOR-targeted therapeutics: Advancements in glioblastoma treatment, International journal of molecular sciences 24 (2023) 14960.

[38] G. Chandrika, K. Natesh, D. Ranade, A. Chugh, P. Shastry, Suppression of the invasive potential of Glioblastoma cells by mTOR inhibitors involves modulation of NFκB and PKC-α signalling, Scientific reports 6 (2016) 22455.

[39] Z. Zou, T. Tao, H. Li, X. Zhu, mTOR signaling pathway and mTOR inhibitors in cancer: progress and challenges, Cell & bioscience 10 (2020) 31.

[40] J. Ren, S. Zheng, L. Zhang, J. Liu, H. Cao, S. Wu, Y. Xu, J. Sun, MAPK4 predicts poor prognosis and facilitates the proliferation and migration of glioma through the AKT/mTOR pathway, Cancer Medicine 12 (2023) 1624-11640.

[41] B. Lawal, C.Y. Lee, N. Mokgautsi, M.R. Sumitra, H. Khedkar, A.T. Wu, H.S. Huang, mTOR/EGFR/iNOS/MAP2K1/FGFR/TGFB1 are druggable candidates for N-(2, 4-difluorophenyl)-2′, 4′-difluoro-4-hydroxybiphenyl-3-carboxamide (NSC765598), with consequent anticancer

implications, Frontiers in Oncology 11 (2021) 656738.

[42] R.S. McNeill, D.A. Canoutas, T.J. Stuhlmiller, H.D. Dhruv, D.M. Irvin, R.E. Bash, S.P. Angus, L.E. Herring, J.M. Simon, K.R. Skinner, J.C. Limas, Combination therapy with potent PI3K and MAPK inhibitors overcomes adaptive kinome resistance to single agents in preclinical models of glioblastoma, Neuro-oncology 19 (2017) 1469-1480.

[43] B. Cheaney, S. Bowden, K. Krause, E.A. Sloan, A. Perry, D.A. Solomon, S.J. Han, M.D. Wood, An unusual recurrent high-grade glioneuronal tumor with MAP2K1 mutation and CDKN2A/B homozygous deletion, Acta neuropathologica communications 7 (2019) 1-4.